Available online at www.sciencedirect.com
SCIENCE DIRECT®
Polymer 45 (2004) 3249–3256
polymer
www.elsevier.com/locate/polymer

Effects of the degree of undercooling on flow induced crystallization in polymer melts

Salvatore Coppola[a], Luigi Balzano[a], Emilia Gioffredi[b], Pier Luca Maffettone[b], Nino Grizzuti[a,*]

[a]*Dipartimento di Ingegneria Chimica, Laboratorio 'Giovanni Astarita', Università degli Studi di Napoli 'Federico II', Piazzale V. Tecchio, 80-80125 Napoli, Italy*

[b]*Dipartimento di Scienza dei Materiali ed Ingegneria Chimica, Politecnico di Torino, Corso Duca degli Abruzzi 24, 10129 Torino, Italy*

Received 25 October 2003; received in revised form 3 March 2004; accepted 11 March 2004

Abstract

This study investigates the coupled effects of mild shear flow and temperature on the crystallization behavior of two thermoplastic polymers, namely, an isotactic polypropylene and an isotactic poly(1-butene). Rheological experiments are used to measure the crystallization induction time under isothermal, steady shear flow conditions. The experimental results clearly show the effects of the degree of undercooling on flow-induced crystallization (FIC). As temperature decreases, the corresponding increase in chain orientation at a given shear rate leads to an *absolutely* faster crystallization. At the same time, however, a temperature decrease makes the flow-induced driving force to crystallization *relatively* less influent with respect to the intrinsic kinetics. A FIC model based on the Doi–Edwards micro-rheological theory is shown to successfully describe the quantitative details of the observed experimental behavior.

Keywords: Flow-induced crystallization; Thermoplastic polymers; Rheology

1. Introduction

The crystallization behavior of thermoplastic polymers is strongly affected by process conditions. The degree of crystallization and the size of the resulting spherulites depend on both temperature and temperature rate of change. Furthermore, flow is known to significantly enhance the kinetics of crystallization and to produce highly oriented morphologies. The global effect of flow on crystallization is often referred to as flow-induced crystallization (FIC).

The dependence of quiescent isothermal crystallization kinetics upon temperature has been widely studied [1–6]. In their fundamental work, Hoffman et al. [5] stated the existence of three temperature ranges or 'regions', corresponding to different temperature dependencies of the nucleation rate. More recently, Ziabicki [7,8] proposed a new, generalized theory. An important extension of this theory is the attempt to account for time dependent external conditions by considering the effects of variable fields (e.g., temperature, pressure, electric or magnetic fields, flow field) on crystallization. To this end, an additional, 'athermal' contribution to nucleation is added due to time-varying fields. The 'thermal' part, conversely, assumes the classical, isothermal form [4]:

$$\dot{N} = Ck_{\mathrm{B}}T\Delta G \exp\left(-\frac{E_{\mathrm{a}}}{k_{\mathrm{B}}T}\right)\exp\left(-\frac{K}{T(\Delta G)^n}\right) \tag{1}$$

In Eq. (1), T is the absolute temperature, k_{B} the Boltzmann constant, K a constant containing energetic and geometrical factors of the crystalline nucleus, n accounts for the temperature region where the homogeneous nucleation takes place, ΔG is the volumetric free energy difference between liquid and crystalline phase, E_{a} the activation energy of the supercooled liquid nucleus interface. The first exponential takes into account the diffusion of chain segments towards the crystallizing germ, while the second term accounts for the driving force of nucleation.

Along with quiescent polymer crystallization, many experimental studies pointed out the major role of flow in the enhancement of crystallization kinetics (for an extensive review see [9]). Quantitative measurements of FIC are quite common in the literature, especially for the case of mild shear flow fields [10–14]. Conversely,

* Corresponding author. Tel.: +39-81-768-2285; fax: +39-81-239-1800.
E-mail address: nino.grizzuti@unina.it (N. Grizzuti).

0032-3861/$ - see front matter © 2004 Elsevier Ltd. All rights reserved.
doi:10.1016/j.polymer.2004.03.049

modeling the interactions between flow and crystallization still remains at a relatively primitive stage. One of the first models of FIC was proposed by McHugh [15]. He proposed that the same expression for the quiescent nucleation rate (Eq. (1)) could be also used under flow, with the assumption that the interface process between liquid and crystalline phase was only modified in the driving force term. In particular the free energy jump included a flow-induced term, which was calculated by using the FENE-P micro-rheological model.

More recently, several phenomenological models have been proposed to predict the influence of flow on crystallization kinetics [16–20]. A major advantage of these models is the possibility to apply them to actual process conditions. A price to be paid, however, is the determination of several adjustable parameters.

Models that describe the effect of flow on a molecular basis seem to be promising [15,21,22]. They are expected to be more robust, as they are developed within a sound physical framework. Furthermore, such models can be fully predictive, as in principle they contain no adjustable parameters. Their often complex mathematical architecture, however, can be a major drawback.

FIC molecular models share the common physical intuition that flow induces local orientations of polymer chains, thus enhancing the nucleation rate. In this regard, temperature plays an important role in that it affects the polymer relaxation times. Indeed, under prescribed flow field, higher temperatures determine lower relaxation times and thus lower orientations. This fact, together with the intrinsic temperature effects on quiescent crystallization kinetics, determines a significant coupling between temperature and flow even under isothermal conditions, i.e., when temperature does not change with time. To our knowledge, this point has never been explicitly considered in FIC models.

Our group has recently proposed a FIC model based on the theory of Doi and Edwards [22,23]. Predictions compare quantitatively well with experimental measurements of isothermal steady shear FIC available in the literature. In this paper we show how the Doi–Edwards micro-rheological model [24], coupled with the classical expression for nucleation rate (Eq. (1)), can be used to describe the combined temperature and flow effects on the early stages of polymer isothermal crystallization.

In the following we first present experimental data that clearly demonstrate the effects of temperature and flow on crystallization kinetics. Experimental evidence provides a physical basis to understand the effects of temperature on isothermal crystallization in the presence of flow. Subsequently, the Doi–Edwards model and the crystallization model will be illustrated and implemented to quantitatively describe the observed experimental features.

2. Materials and methods

In this work, an isotactic polypropylene (*i*-PP T30G produced by Montell) and an isotactic poly (1-butene) (*i*-PB 200 produced by Shell) were used. Some relevant properties of the polymers are shown in Table 1.

The linear viscoelastic characterization of the two polymers can be found elsewhere [25,26]. As it will be shown later, in order to obtain quantitative predictions from the model, several parameters are required: the longest relaxation time, τ_{max}, the viscoelastic activation energy, $\Delta E/R$, the molecular weight between entanglements M_e, the crystallization parameter, K_n (see Eq. (1)). All these parameters were either extracted from the literature or independently measured. In particular, M_e of *i*PB was determined from linear viscoelastic characterization by estimating the plateau value of the storage modulus [24]. The crystallization parameter K_n was determined from DSC quiescent data [27].

Rheological measurements were performed on two stress-controlled rotational rheometers, a SR-200 rheometer (Rheometric Scientific Inc.), and a AR500 (TA Instruments). The SR 200 rheometer was equipped with cone and plate fixtures (cone angle 0.1 rad, 25 mm diameter), while for the AR500 parallel plates were used (25 and 40 mm diameters). Some experiments on the SR-200 rheometer were also performed with a homemade 13 mm diameter, parallel plate system. Although less accurate in view of the shear rate distribution between the plates, the parallel plate configuration allowed for the application of higher shear stresses.

Disc-shaped samples of *i*PB and *i*PP were prepared from the as-received pellets by compression molding at 160 °C (*i*PB) and 240 °C (*i*PP) for 10 min. Samples were always pre-heated in the rheometer to 160 °C (*i*PB) or 240 °C (*i*PP) for 15 min in order to guarantee a complete melting of the crystalline phase. Measurements were carried out under a dry nitrogen atmosphere to minimize polymer degradation.

3. Experimental results

A rather common characterization of the crystallization kinetics under flow is based on the so-called induction time, that is, the time required for the onset of crystallization. Typically, in isothermal experiments at imposed shear rate, the time corresponding to a sudden upturn of the shear viscosity is considered [10–12]. Here, we use the same procedure to produce data comparable with the predictions of our model. The latter is indeed valid just in the early stages of crystallization and can be then used only to predict the induction time. Therefore, the following experimental protocol was adopted. After the high temperature annealing, the sample is cooled down (−10 °C/min) to the desired crystallization temperature, T_c ($T_c < T_m^0$, where T_m^0 is the thermodynamic melting temperature). Then a constant

Table 1
Material properties of *i*PPT30g and PB200

	M_n (g/mol)	M_w (g/mol)	M_w/M_n	MFI (dg/min)	*mmmm* (%)	T_m^0 (°C)	η_0 (Pa s)
*i*PP T30G	55,600	376,000	6.76	3.6	87.6	194	8000[a]
PB 200	106,000	398,000	3.8	1.8	82.7	138	41,780[b]
	τ_{max} (s)	$\Delta E/R$ (K)	H_0 (j/m^3)	n	K (K(j/m^3)^n)	ρ (kg/m^3)	M_e (g/mol)
*i*PP T30G	10[a,c]	5020	1.4×10^8	1	9.0×10^{10}	970	4620[d]
PB 200	250[b,c]	5180	6.54×10^7	1	2.9×10^{10}	914	18,400[c]

[a] At $T_{ref} = 230$ °C.
[b] At $T_{ref} = 140$ °C.
[c] From linear viscoelasticity [25].
[d] From Ref. [28].

stress, σ, is applied and the polymer viscosity is monitored. A viscosity induction time, ϑ, is determined as the time corresponding to a sudden rise in the viscosity with respect to its initial steady state value.

For both materials, experiments were carried out at two different crystallization temperatures, namely, 98 °C and 105 °C (*i*PB), 140 °C and 160 °C (*i*PP). The choice of the two test temperatures for each material was dictated by two important constraints. On the one hand, temperatures were chosen so as to determine measurable induction times. In fact, too high temperatures (close to T_m^0) result in very low crystallization rates, whereas too low temperatures cause an essentially instantaneous crystallization. In both cases, the measurement of the induction time becomes impossible, or at best unreliable. On the other hand, the two temperatures were chosen so as to determine the largest possible difference in the induction time, in order to guarantee the highest amplification of the temperature effects. Other experimental measurements of induction times at different temperatures under a steady shear flow can be found in the literature [10,11]. In these cases, however, the temperature range explored was always too narrow, thus making impossible to observe the peculiar effects of temperature on FIC that will be described below.

Typical flow induced crystallization results are shown in Figs. 1 and 2. In Fig. 1, data refer to PB200 at 98 °C, whereas Fig. 2 is for *i*PPT30G at 140 °C. Crystallization is easily detected when a sudden rise of viscosity (normalized to its initial, steady state value η_{ss}) is observed. Induction times become shorter as the stress increases, a signature of flow induced crystallization.

The experimentally determined induction times for the two polymers are reported in Figs. 3 and 4 as a function of the applied shear rate. It should be pointed out that shear rate has been chosen as a flow parameter although experiments have been carried out at constant shear stress. In fact, shear rate and shear stress are equivalent as long as one considers the early stages of crystallization, because viscosity has not yet changed significantly.

As expected, a significant enhancement of the crystallization kinetics is observed upon increasing the flow intensity. Obviously, larger induction times are observed at higher temperatures, that is, closer to the thermodynamic melting point. The relevant change of crystallization kinetics with temperature can be appreciated. For PB200, a change of only 7 °C in temperature produces almost a factor of ten difference in the induction time. For *i*PPT30G, a decrease in 20 °C in the crystallization temperature generates a two order of magnitude acceleration in the crystallization kinetics.

The data of Figs. 3 and 4 show also that FIC is active only above a critical value of shear rate, $\dot{\gamma}_c$. This is an expected

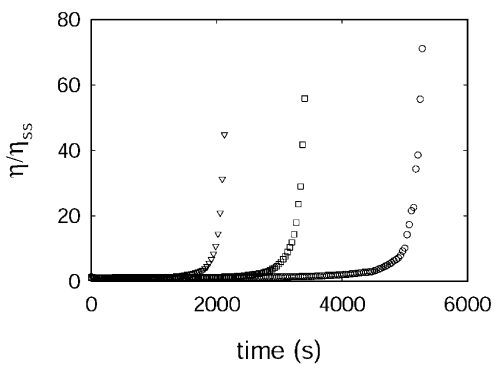

Fig. 1. The normalized viscosity of PB200 at $T_c = 98$°C as a function of time for different applied shear stresses. (○) $\sigma = 1000$ Pa; (□) $\sigma = 3160$ Pa; (▽) $\sigma = 10,000$ Pa.

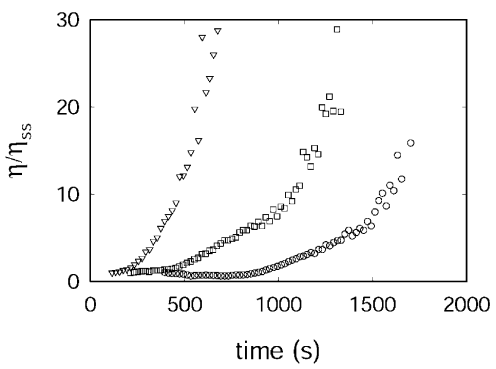

Fig. 2. The normalized viscosity of *i*PPT30G at $T_c = 140$ °C as a function of time for different applied shear stresses. (○) $\sigma = 238$ Pa; (□) $\sigma = 477$ Pa; (▽) $\sigma = 795$ Pa.

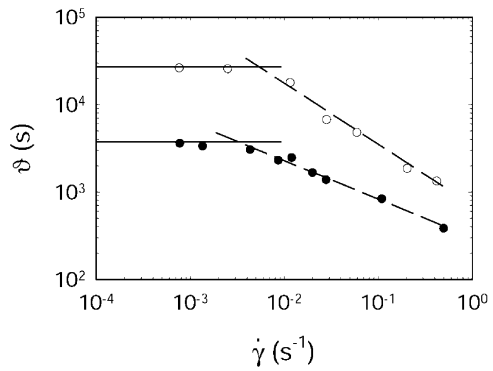

Fig. 3. The induction time of PB200 as a function of shear rate. (●) T_c = 98 °C; (○) T_c = 105 °C. Solid lines indicate the quiescent induction time, dashed lines are a linear fit of the high shear rate data.

result, if the idea that the enhancement in crystallization is related to polymer chain orientation in the melt is accepted. A temperature increase determines a decrease in the polymer relaxation time, that is, a lower degree of orientation under the same shear rate. As a consequence, $\dot{\gamma}_c$ is expected to increase as temperature increases. This trend is quite clear from Figs. 3 and 4.

A quantitative estimate of the critical shear rates at the different temperatures was made by determining the intersection of the horizontal straight line defining the quiescent induction time (solid lines in Figs. 3 and 4) with the best linear fit of the induction time data at the higher shear rates (dashed lines). The results are summarized in Table 2, where the longest relaxation times, τ_{max}, of each polymer are also reported. The values of τ_{max} at any temperature have been determined by using the activation energies obtained from viscoelastic measurements and reported in Table 1. By changing temperature, the product of the critical shear rate and of the maximum relaxation time remains essentially constant for each polymer. Such a product represents a critical Deborah number (always of order unity) for the FIC process. It confirms that FIC is driven by chain orientation.

The effect of temperature on the crystallization kinetics does not reflect only in a change of the critical shear rate. A

Table 2
The critical shear rate, the maximum relaxation time and the critical Deborah number for *i*PPT30G and PB200 at the different crystallization temperatures

	T (°C)	$\dot{\gamma}_c$ (s^{-1})	τ_{max} (s)	$De_c = \dot{\gamma}_c \tau_{max}$
PB200	98	3.8×10^{-3}	1030	3.9
	105	5.4×10^{-3}	800	4.3
*i*PPT30G	140	4.8×10^{-2}	88	4.2
	160	7.0×10^{-2}	50	3.5

closer inspection of Figs. 3 and 4 reveals that the slope of the induction time vs. shear rate is steeper at higher crystallization temperatures. This fact is made clearer when the data are normalized to their relative quiescent value at each crystallization temperature. To this end, a dimensionless induction time is introduced:

$$\Theta \equiv \frac{\vartheta_f}{\vartheta_q} \tag{2}$$

where ϑ_f and ϑ_q are the induction times under flow and quiescent conditions, respectively. Obviously, $\Theta = 1$ under quiescent conditions, whereas $\Theta \leq 1$ when flow is applied.

The dimensionless induction times for *i*PB and *i*PP are plotted in Figs. 5 and 6. Another set of experimental data for *i*PPT30G, already published elsewhere [22] has been also added for comparison. For both polymers, a more pronounced sensitivity of the induction time to flow intensity is found at the higher temperature. In other words, the slower the crystallization in quiescent conditions, the more pronounced is the *relative* effect of flow. This fact can be again physically interpreted in terms of polymer chain orientation. As the temperature increases, both the orientational effect of flow and the quiescent crystallization kinetics are depressed. The latter, however, is much more sensitive to temperature. Furthermore, while the intrinsic crystallization rate (i.e., in the absence of flow) tends to zero as the temperature approaches the thermodynamic melting point, the flow-induced orientation effect survives at any temperature. As a consequence, the relative effect of flow in

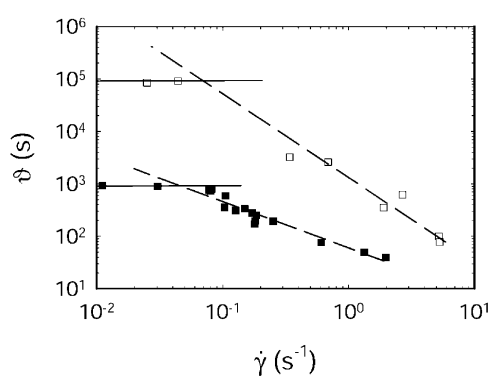

Fig. 4. The induction time of *i*PPT30G as a function of shear rate. (■) T_c = 140 °C; (□) T_c = 160 °C. Lines as in Fig. 3.

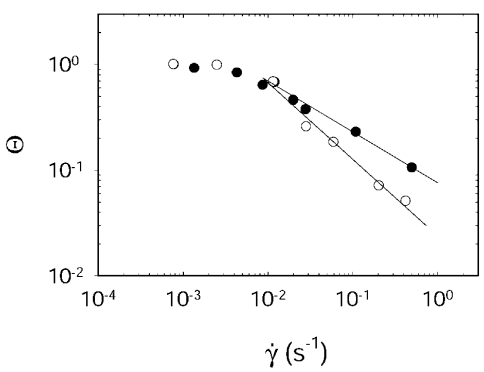

Fig. 5. Dimensionless induction time data for PB200. Symbols as in Fig. 3. The lines through the data are only to guide the eye.

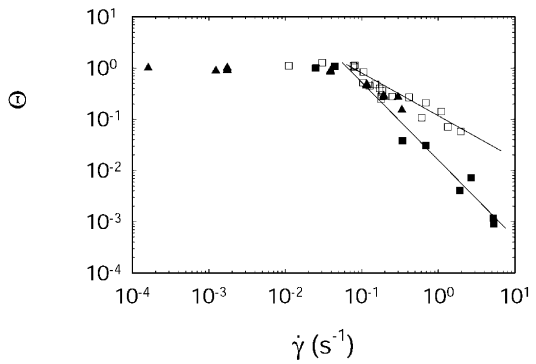

Fig. 6. Dimensionless induction time data for *i*PPT30G. Symbols as in Fig. 4. Additional data (from Ref. [22]) have been added (▲). The lines through the data are only to guide the eye.

enhancing the kinetics becomes more pronounced as the degree of undercooling decreases. This point will find a more quantitative confirmation in the following section.

3.1. Model

The model for FIC used in this work is summarized in the following. Further details on the model can be found elsewhere [22,23].

The model assumes that the effect of flow is mainly localized in the nucleation stages, as often verified experimentally [29]. A further assumption is that the effect of flow on the nucleation rate is merely additive, thus reflecting in an increase in the thermodynamic driving force for nucleation. Under these assumptions, the free energy difference between liquid and crystalline phase appearing in Eq. (1) is modified as follows:

$$\Delta G = \Delta G_q + \Delta G_f \tag{3}$$

where ΔG_q is the quiescent free energy change at the crystallization temperature and ΔG_f the flow-induced free energy change of the melt phase.

The explicit expression for ΔG_f is derived from the micro-rheological model of Doi and Edwards [24]. In particular, if the so-called independent alignment approximation (IAA) variant of the model is used, the flow-induced excess free energy assumes a relatively simple form [30]:

$$\Delta G_f = 3ck_BT\int_0^{+\infty}\dot{\mu}(z)A(\mathrm{De}z)\mathrm{d}z \tag{4}$$

In Eq. (4), c is the entanglement density:

$$c = \frac{\rho\mathcal{N}}{M_e} \tag{5}$$

where ρ is the melt density, $\mathcal{N}$ is the Avogadro number, and M_e the molecular weight between entanglements [24]. $A(x)$ is a known integral function of the deformation history that, for steady-state shear flow, is given by:

$$A(x) = \frac{1}{2}\int_0^1 \ln\left(\frac{1+x^2\xi^2+\sqrt{\xi^4(x^4+4x^2)-2x^2\xi^2+1}}{2}\right)\mathrm{d}\xi \tag{6}$$

μ is the Doi–Edwards memory function:

$$\mu(t,t') = \frac{8}{\pi^2}\sum_{p\ \mathrm{odd}}\frac{1}{p^2}\exp\left[-\frac{p^2(t-t')}{\tau_d}\right] \tag{7}$$

where τ_d is the disengagement time. De is the Deborah number, which is defined as the ratio between the disengagement time and the flow characteristic time:

$$\mathrm{De} = \tau_d\dot{\gamma} \tag{8}$$

The set of Eqs. (1) and (3)–(8) can be used to calculate the induction time assuming, as often made in the literature [10,12], that the induction time is inversely proportional to the nucleation rate:

$$\dot{N} \propto \frac{1}{\vartheta} \tag{9}$$

It is worth noting that, in principle, the model contains no adjustable parameters. In fact, all physical quantities appearing in the model equations can be directly measured from independent experiments. The model summarized above has been already used to successfully predict the induction time of several thermoplastic polymers under isothermal, steady shear flow [22].

In this paper, the emphasis is on the coupled effects of temperature and flow field on the crystallization rate. For this reason, and in view of Eq. (9), the model expression for the dimensionless induction time, introduced in the previous section, is given by:

$$\Theta(T_c,\dot{\gamma}) \cong \frac{\dot{N}_q}{\dot{N}_f} = \frac{1}{1+\dfrac{\Delta G_f}{\Delta G_q}}\exp\left\{\frac{K_n}{T(\Delta G_q)^n}\left[\frac{1}{\left(1+\dfrac{\Delta G_f}{\Delta G_q}\right)^n}-1\right]\right\} \tag{10}$$

where $\dot{N}_f$ and $\dot{N}_q$ are the nucleation rates under flow and quiescent conditions, respectively.

The role of temperature in Eq. (10) is multi-folded, as detailed in the following. Apart from the explicit dependence, temperature appears both in the quiescent and flow-induced free energy terms. The quiescent term, in fact, can be expressed to a good approximation as:

$$\Delta G_q = H_0\left(1-\frac{T_c}{T_m^0}\right) \tag{11}$$

where H_0 is the latent heat of fusion. Obviously, ΔG_q decreases as the degree of undercooling decreases, and becomes rigorously zero at the thermodynamic melting temperature. In the flow term (see Eq. (4)) temperature acts with a weak explicit dependence, but with a strong implicit effect through the Deborah number. At fixed shear rate, as temperature increases the relaxation time decreases, thus De decreases. As already mentioned, this corresponds to the physical concept that less orientation is produced at higher temperatures by a flow of given intensity. From a quantitative point of view, for temperatures well above the polymer glass transition, an Arrhenius-type dependency holds [31]:

$$\tau(T_c) = \tau_0 \exp\left[\frac{\Delta E}{R}\left(\frac{1}{T_c} - \frac{1}{T_0}\right)\right] \tag{12}$$

where T_0 and τ_0 are a reference temperature and a reference relaxation time, respectively. From Eqs. (4) and (12) it can be concluded that also the flow-induced free energy term is a decreasing function of temperature. Unlike ΔG_q, however, ΔG_f does not vanish at the thermodynamic crystallization temperature: flow imparts orientation at any temperature.

The coupled effect of temperature and flow on the dimensionless induction time can now be revisited. As shown by Eq. (10), Θ strongly depends on the ratio $\Delta G_f/\Delta G_q$. At fixed temperature, the only parameter that can be used to modify this quantity is flow intensity. As the shear rate is increased the ratio becomes larger and Θ decreases, as expected. If the flow intensity is imposed, an increasing temperature also increases the ratio, and again Θ decreases accordingly. Notice that $\Delta G_f/\Delta G_q$ diverges at the melting point. In this case Eq. (10) informs that Θ becomes zero for any non-zero value of the shear rate. In any event, only the *relative* effect of flow on the crystallization rate becomes increasingly important as the thermodynamic melting point is approached. Obviously, the *absolute* rate of crystallization at any shear rate remains an increasing function of the degree of undercooling.

It should be stressed that the above arguments are not restricted by the choice of a specific rheological model, as long as the general concept that flow increases the free energy of the melt is accepted. In order to give a quantitative form to the model predictions, the Doi–Edwards model has been implemented over a wide range of shear rates and crystallization temperatures by using the physical parameters of the isotactic poly(1-butene) PB200 given in Table 1. The results are summarized in Fig. 7, where the predicted induction time is reported as a function of both shear rate and temperature. Fig. 7 confirms that, while the induction time at a given shear rate is predicted to be always smaller at higher degrees of undercooling, the relative drop of the flow-induced induction time is much more dramatic as the temperature approaches the thermodynamic crystallization point.

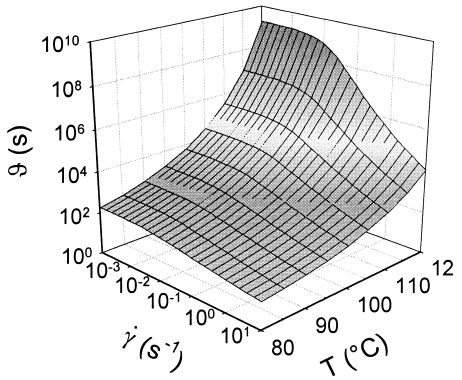

Fig. 7. The induction time as a function of shear rate and crystallization temperature. Predictions of the D–E model are obtained by using the material properties of PB200.

3.2. Model validation

In this section the predictions of the model are validated against the experimental data for FIC previously presented. As already mentioned, all parameters of the model can be obtained by independent experiments. The model, therefore, contains no adjustable parameters. Problems can arise, however, when estimating the disengagement time. This is mainly due to the polydispersity of the polymer sample, whereas the D–E theory assumes monodispersity. This problem has been already considered elsewhere [22]. For this reason, in the following comparison only one adjustable parameter is used, i.e., the polymer relaxation time τ.

Fig. 8 shows again the experimental data for PB200 at the two different temperatures, along with model predictions. For this polymer an estimate of the disengagement time can be extracted from the experimental data as the inverse of the largest frequency where the $G'(\omega)$ curve has a slope equal to 2 in a log–log plot [24]. This amounts to set $\tau_d \cong \tau_{max}$, where τ_{max} is the polymer longest relaxation time. A shift of τ_{max} from 140 °C (see Table 1) to 98 °C by using the experimentally available activation energy (see again Table 1), yields a disengagement time of about 1000 s at 98 °C. The best fit of the model at 98 °C, conversely, provides a value of $\tau \cong 500$ s, which compares well with the above

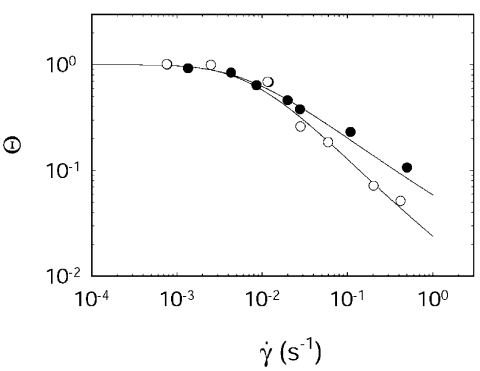

Fig. 8. The dimensionless induction time of PB200 as a function of shear rate. Symbols denote experimental data as in Fig. 5. Solid lines are predictions of the model.

experimental value. Fig. 8 shows the good agreement between model and experiments with only one adjustable parameter. The agreement is even more remarkable when considering that the relaxation time fit was done only at 98 °C. The value at 105 °C used in the model was obtained by the time–temperature shift procedure.

Good agreement between model and experiments is also found for the *i*PPT30G, as shown in Fig. 9. Also in this case the single parameter fit involves only one set of data at one temperature (140 °C). As for PB200, the relaxation time at the other temperature (160 °C) has been obtained by means of a temperature shift based on the independently measured activation energy. Unlike PB200, for *i*PP the terminal region where the storage modulus is quadratic with frequency could not be reached, also due to the larger polydispersity of this polymer. Then it was not possible to estimate the disengagement time directly from linear viscoelastic characterization. It is however useful to remark that the relaxation time fitted with the model ($\tau = 40$ s) is not too different from the longest relaxation time obtained by fitting the $G'(\omega)$ curve with a multi-modes Maxwell model at the reference temperature (see Table 1). The subsequent shift to the experimental temperature of 140 °C gave a $\tau_{max} \cong 100$ s. Also in this case, therefore, the experimental and the model best fit relaxation times are in the same order of magnitude. It should be noticed that in both cases the experimental longest relaxation time is always larger by a factor of about two than the one that allows the best model fit.

4. Concluding remarks

We believe that the main conclusion of this paper is that the role of temperature on the FIC of thermoplastic polymers has been more explicitly clarified. Both model and experiments indicate that the degree of undercooling plays a complex role. When temperature moves down away from the thermodynamic melting point, the 'intrinsic' kinetics (i.e., the quiescent crystallization rate) are strongly accelerated. When flow is present, two further concurrent effects must be considered. On the one hand, to a temperature decrease it corresponds an increase in the relaxation time. In turn, this increases the degree of orientation of the polymer chains at a given shear rate, thus leading to an *absolutely* faster crystallization. On the other hand, a temperature decrease makes the flow-induced driving force to crystallization *relatively* less influent with respect to the intrinsic kinetics. This second effect is particularly intriguing. In fact, the general, model-independent conclusion is that the *relative* effect of flow on crystallization becomes more and more dramatic as the temperature approaches the thermodynamic limit. From this point of view, a closer look at the model results reported in Fig. 7 is particularly illuminating. We remind that this figure is a 'model simulation' of the PB200 crystallization behavior. Let us take, for example, a temperature of 100 °C and a shear rate of 10 s^{-1}. The latter corresponds to a shear stress of 0.065 MPa. The predicted induction time is about 100 s. If the temperature is now lowered to 80 °C, the same shear stress would produce a shear rate of 4.5 s^{-1}, and an induction time of about 25 s, that is, in the same order of magnitude of the one obtained at the higher temperature under the same shear stress. Fig. 7 also informs, however, that the quiescent induction time is 6200 s at 100 °C and 180 s at 80 °C. This means that the quiescent kinetics change by a factor of 35 between 80 and 100 °C, whereas the flow induced kinetics change, within the same temperature difference, only by a factor of 4 if the same stress is applied to the material. At both temperatures the induction time is approaching a similar value. As a consequence, in both cases crystallization can be considered similarly fast. It should be noticed that this physical picture is consistent with experimental observations by Lagasse and Maxwell [10] on polyethylene and by Tribout et al. [12] on an ethylene–propylene block copolymer. They both found a nearly temperature-independent nucleation rate when a high shear flow was applied to the polymer. More recently, Kumaraswamy et al. [32] observed extremely high crystallization rates for an isotactic polypropylene under process conditions even at temperatures close to the melting point when high stresses are imposed to the polymer.

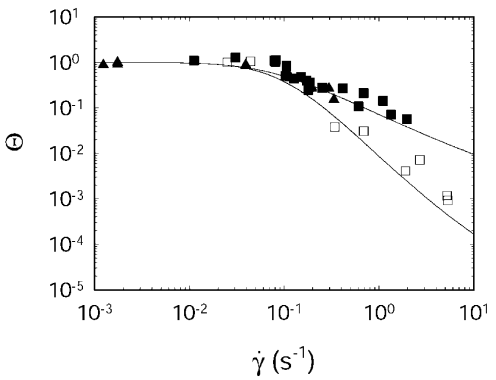

Fig. 9. The dimensionless induction time of *i*PPT30G as a function of shear rate. Symbols denote experimental data as in Fig. 6. Solid lines are predictions of the model.

The comparison between the experimental data and the crystallization model based on the Doi–Edwards micro-rheological theory is particularly encouraging. Good quantitative agreement is reached with only one adjustable parameter, a characteristic relaxation time of the polymer at one single temperature. The model does not account for polydispersity but, as shown, it works sufficiently well also for significantly polydisperse samples. Further experimental and theoretical work in this direction could carry some improvement to the model. In any event, the model can be implemented under arbitrary flow histories, calling for its direct validation into simulation codes describing FIC in more complex, process-oriented flow conditions.

Acknowledgements

The authors wish to thank G.C. Alfonso for providing DSC data.

References

[1] Avrami M. J Chem Phys 1939;7:1103.
[2] Avrami M. J Chem Phys 1940;8:212.
[3] Avrami M. J Chem Phys 1941;9:177.
[4] Turnbull D, Fisher JC. J Chem Phys 1949;17:71.
[5] Hoffman JD, Weeks JJ, Murphey WM. J Res Natl Bur Stand 1959; 63A:67.
[6] Lauritzen JI, Hoffman JD. J Res Natl Bur Stand 1960;64A:73.
[7] Ziabicki A. Colloid Polym Sci 1996;274:209.
[8] Ziabicki A. Colloid Polym Sci 1996;274:705.
[9] Kornfield JA, Kumaraswamy G, Issaian AM. Ind Engng Chem Res 2002;41:6383.
[10] Lagasse RR, Maxwell B. Polym Engng Sci 1976;16:189.
[11] Nieh J, Lee L. J Polym Engng Sci 1998;38:1121.
[12] Tribout C, Monasse B, Haudin JM. Colloid Polym Sci 1996;274:197.
[13] Somani RH, Hsiao BS, Nogales A, Srinivas S, Tsou AH, Sics I, Balta-Calleja FJ, Ezquerra TA. Macromolecules 2000;33:9835.
[14] Bove L, Nobile MR. Macromol Symp 2002;185:135.
[15] McHugh AJ. Polym Engng Sci 1982;22:15.
[16] Eder G, Janeschitz-Kriegl H. In: Meijer HEH, editor. Structure development during processing: crystallization. Materials science and technology, vol. 18. Weinheim: Verlag Chemie; 1997. p. 269–342.
[17] Zuidema H, Peters GWM, Meijer HEH. Macromol Theory Simul 2000;10:447.
[18] Doufas AK, Dairanieh IS, McHugh AJ. J Rheol 1999;43:85.
[19] Doufas AK, McHugh AJ, Miller CJ. J Non-Newtonian Fluid Mech 2000;92:27.
[20] Doufas AK, McHugh AJ, Miller C, Immanemi A. J Non-Newtonian Fluid Mech 2000;92:81.
[21] Ziabicki A, Jarecki L. In: Ziabicki A, Kawai H, editors. High-speed fiber spinning. New York: Wiley; 1985. p. 225–65.
[22] Coppola S, Grizzuti N, Maffettone PL. Macromolecules 2001;34: 5030.
[23] Acierno S, Coppola S, Grizzuti N, Maffettone PL. Macromol Symp 2002;185:233.
[24] Doi M, Edwards SF. The theory of polymer dynamics. Oxford: Clarendon Press; 1986.
[25] Acierno S, Palomba B, Grizzuti N, Winter HH. Rheol Acta 2003;42: 243.
[26] Acierno S, Grizzuti N. J Rheol 2003;47:563.
[27] Alfonso GC. Personal communication; 2003.
[28] Fetters LJ, Lohse DJ, Richter D, Witten TA, Zirkel A. Macromolecules 1994;17:4639.
[29] Liedauer S, Eder G, Janeshitz-Kriegl H, Jershow P, Geymayer W, Ingolic E. Intern Polym Process 1993;VIII:236.
[30] Marrucci G, Grizzuti N. J Rheol 1983;27:433.
[31] Ferry J. Viscoelastic properties of polymers. New York: Wiley; 1980.
[32] Kumaraswamy G, Kornfield JA, Yeh F, Hsiao BS. Macromolecules 2002;35:1762.